Available online at www.sciencedirect.com
SCIENCE DIRECT®
ELSEVIER
Nuclear Instruments and Methods in Physics Research A 520 (2004) 512–515
NUCLEAR INSTRUMENTS & METHODS IN PHYSICS RESEARCH Section A
www.elsevier.com/locate/nima

A 12 × 10 pixels superconducting tunnel junction array based spectro-photometer for optical astronomy

D.D.E. Martin*, P. Verhoeve, A. Peacock, A. van Dordrecht, J. Verveer, R. Hijmering

Science Payload and Advanced Concepts Office of the European Space Agency, ESTEC, Keplerlaan 1, Noordwijk 2201 AZ, The Netherlands

Abstract

Superconducting Tunnel Junctions (STJs) have been extensively investigated as photon detectors covering the range from near-infrared to X-ray energies. A 6 × 6 array of Ta junctions has already been used in an optical spectro-photometer. With this camera, the European Space Agency has performed multiple astronomical observations of optical sources using the William Herschel 4.2 m telescope at La Palma. Following the success of this programe, we are now completing the development of a second generation camera. The goals of this programe were to increase the field of view of the instrument from 4'' × 4'' to 11'' × 9'', to optimize IR rejection filters (possibly extending the 'red' response to ~1 μm), and to increase the electronics readout speed. For these purposes, we have developed a new STJ array consisting of 10 × 12 Ta/Al devices as well as an improved readout system. In this paper, we review the instrument's architecture and describe the performance of the new detector array.

PACS: 85.25; 07.60.R; 42.50.A

Keywords: Superconducting tunnel junctions; Arrays; Imaging; Spectrograph; Astronomy

1. Introduction

The present generation of detectors in UV/optical astronomy ($\lambda \sim 100$–1000 nm or $E = 1.2$–12 eV) is based on semiconductors (CCDs) or micro-channel plates (MCPs). CCDs combine large sensitive area (several cm^2) with high-resolution imaging and excellent quantum efficiency (QE) in the optical, but no photon-counting capability and marginal QE for $\lambda < 300$ nm. In the UV, MCPs are most widely used because of the better QE of 10–40%, depending on wavelength and photo-cathode material. In addition, they provide photon-counting capability with time resolution < 1 μs.

Recent developments in cryogenic detectors, such as superconducting tunnel junction (STJ) arrays [1,2], have added a third dimension to UV/optical detectors: simultaneous with the position information, they can provide each photon's arrival time and wavelength. Combined with their high detection efficiency (50–70% over the range

*Corresponding author. Tel.: +31-71-5653557; fax: +31-71-5654690.

E-mail address: didier.martin@esa.int (D.D.E. Martin).

0168-9002/$ - see front matter © 2003 Elsevier B.V. All rights reserved.
doi:10.1016/j.nima.2003.11.301

$\lambda \sim 115$–700 nm), this makes them the ideal detectors for applications such as fast spectro-photometry or deep-field imaging. The performance of current STJ arrays allows the simultaneous measurement of broadband low-resolution spectra of very faint extragalactic sources to be obtained for all objects in the field. Such spectra containing emission line complexes or continuum absorption features (the Lyman edge) in very faint extragalactic objects have already allowed the direct determination of redshifts [3].

2. The S-CAM programe

The S-Cam programme consists of the development, in a phased approach, of a superconducting camera for ground-based optical astronomy. The original S-Cam1 (a simple technology demonstrator) and S-Cam2 were designed around a 6×6 array of Ta/Al STJs [4,5]. The optical collimator was designed to interface the camera's focal plane to the Nasmyth focus of the Ground High-Resolution Imaging Laboratory of the William Herschel Telescope at La Palma.

Following the successes of the original S-Cam2 observing campaigns in the period 1999–2000, we decided to improve the system to achieve the following goals:

- Increase the field-of-view from $4'' \times 4''$ to $11'' \times 9''$.
- Optimize IR rejection filters, possibly extending the 'red' response to $\sim 1\,\mu$m.
- Increase the energy resolution.
- Increase the electronics readout speed and hence the system's photon rate capability.
- Improve the data acquisition software robustness.

2.1. IR optimization

The rejection of thermal infrared photons is of crucial importance. The low-energy gap of Ta/Al STJs (520 μeV) makes them sensitive to wavelengths up to ~ 1 mm. Since the detector is optically coupled to a 300 K environment, the IR rejection filters have very tight requirements. In S-Cam2 this problem was solved by baffling and by using KG2 and KG5 glasses from Schott plus a 1 mm thick SiO_2 window in front of the detector. However, simple calculations of attenuation factors in the vicinity of the peak of the 300 K blackbody radiation could not explain the excess in sub-gap current (~ 0.4 nA or 0.6 pA/μm^2) measured with our detectors. We concluded that we were suffering from residual very long-wavelength radiation. In order to suppress this even further, we replaced the innermost filters (KG5 and SiO_2) by 10 mm thick BK7 glasses [2]. With a more careful baffling, this resulted in an order of magnitude reduction in IR load as well as a better transmission efficiency. Fig. 1 shows the resulting curves, which take into account the measured transmissions of all optical elements as well as the detector's efficiency. Peak efficiency has increased from $\sim 22\%$ in S-Cam2 to $\sim 34\%$ in S-Cam3. The bandwidth (at 1% transmission) also increased from 340–720 nm to 330–800 nm.

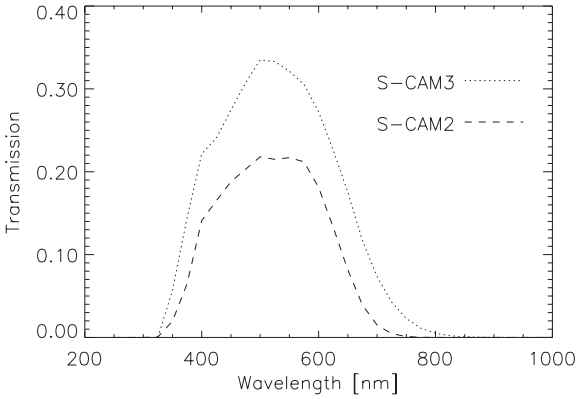

Fig. 1. Measured optical transmission curves (including the detector's efficiencies) for S-Cam2 (dashed) and S-Cam3 (dotted).

2.2. Pulse processing

Traditionally, pulse processing has been achieved by using analog semi-Gaussian shaping filters. The purpose of these filters is two-fold; they reduce the noise bandwidth to optimize the signal-to-noise ratio and they provide a compact impulse response in order to reduce pile-up as much as possible.

In S-Cam3, we have chosen to digitize each buffered preamplifier signal at a programmable rate of up to 40 Msamples per second. The digital samples are passed to a finite impulse response (FIR) filter which serves as the shaping stage. The filter's impulse response is very simple in that its tap coefficients are either 1 or –2. By changing the length of the filter (up to 768 taps) and/or the sampling rate, one can change the effective pulse shaping time over several orders of magnitude. In practice, however, the shaping times will be in the range 1–50 μs. This allows us to optimize the settings for speed with a short FIR (lower pile-up probability) or better energy resolution with a longer FIR.

The simplicity of the FIRs (they only require adders and FIFOs) makes it possible to integrate them into FPGAs. Further logic in these chips provides for threshold detection, peak search and sampling, time tagging, a digital pulse generator for electronic noise determination, buffering and the required 'glue'-logic. Every event which passes a programmable threshold gets detected and the pixel address information with a time tag derived from a GPS receiver is forwarded to a fast buffer. The hardware buffer is then read out by a PC using a fast PCI parallel port and logged onto disk.

Separating the data stream into quick-look, with spectra and light-curve accumulation implemented in hardware, and logging alleviated the speed and robustness limitations of the earlier S-Cam2 system. Achieved system throughputs are 10^4 photons/s/pixel and 5×10^5 photons/s for the whole array.

2.3. The detector

The S-Cam3 detector is an array of 10×12 pixels, each $33 \times 33\,\mu m^2$, with 4 μm interpixel gaps. The pixel size corresponds to $\sim 0.8'' \times 0.8''$ on the sky, which is well matched to the seeing conditions at the La Palma observatory.

The large increase in the number of pixels and the moderate increase in pixel size have increased the field-of-view of the instrument from $4'' \times 4''$ in S-Cam2 to $11'' \times 9''$ in the new instrument. This allows for observations even in bad seeing conditions, better background determination and subtraction, and more accurate photometry. Fig. 2 shows a micrograph of the S-Cam3 array.

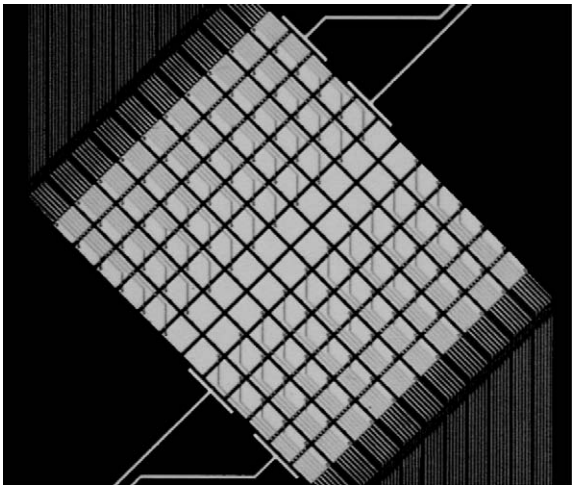

Fig. 2. S-CAM3 array micrograph.

The detectors consist of a sandwich of 100 nm Ta, 30 nm Al, Al_2O_3, 30 nm Al and 100 nm of Ta films and are operated at ~ 300 mK. By optimizing the processing of the devices, we have been able to increase the responsivity from $\sim 15000\,e^-/eV$ in S-Cam2 to $\sim 17000\,e^-/eV$ in the current devices. The increased IR rejection also reduced the sub-gap current, which is now typically 50 pA per pixel (or $\sim 50\,fA/\mu m^2$). With these effects combined, we have been able to measure a resolution $\mathscr{R} = E/\Delta E = 13$ at 500 nm, up from $\mathscr{R} = 8$ in S-Cam2.

Uniformity of the array is sufficient to reduce the Josephson current on all pixels below 50 nA using a ~ 180 Gauss field. The major challenge of biasing simultaneously 120 pixels was achieved by grouping the pixels into 4 sets of 30 detectors each. Each group has its own return line and set of preamplifiers. Stable biasing is obtained in the range of 80–170μV.

3. Conclusions

The S-CAM3 system meets all its objectives with the exception of the 'red' response extension to 1 μm. This limitation comes from the unavailability of IR suppression filters with appropriate wider

band-pass characteristics. The system is now almost fully assembled and will shortly undergo full calibration.

References

[1] A. Peacock, et al., Nature 381 (1996) 135.
[2] D. Martin, et al., Proc. SPIE. 4841 (2003) 805.
[3] M.A.C. Perryman, et al., Mon. Not. R. Astron. Soc. 324 (2001) 899.
[4] N. Rando, et al., Proc. SPIE. 4008 (2000) 646.
[5] P. Verhoeve, et al., Proceedings of LTD7, Munich, 1997, pp. 97–100.